J Mol Neurosci (2016) 59:544–553
DOI 10.1007/s12031-016-0775-y

PPAR-α Agonist WY-14643 Inhibits LPS-Induced Inflammation in Synovial Fibroblasts via NF-kB Pathway

Degang Huang[1] · **Quanlai Zhao**[1] · **Hongfei Liu**[1] · **Yongjie Guo**[1] · **Hongguang Xu**[1]

Received: 11 April 2016 / Accepted: 26 May 2016 / Published online: 24 June 2016

Abstract Osteoarthritis (OA), the most prevalent form of arthritis that results from breakdown of joint cartilage and underlying bone, has been viewed as a chronic condition manifested by persistence of inflammatory responses and infiltration of lymphocytes. Regulation of the inflammatory responses in synovial fibroblasts might be useful to prevent the development and deterioration of osteoarthritis. WY-14643, a potent peroxisome proliferator activator receptor-α (PPAR-α) agonist, has been described to beneficially regulate inflammation in many mammalian cells. Here, we investigate the potential anti-inflammatory role of WY-14643 in lipopolysaccharide (LPS)-induced synovial fibroblasts. WY-14643 greatly inhibited the production of NO and PGE_2 induced by LPS. In addition, the mRNA expression of intracellular adhesion molecule-1 (ICAM-1), vascular cell adhesion molecule-1 (VCAM-1), endothelin-1 (ET-1), and tissue factor (TF) was significantly suppressed by WY-14643, as well as the secretion of pro-inflammatory cytokines including interleukin-6 (IL-6), IL-1β, tumor necrosis factor-α (TNF-α), and monocyte chemotactic protein-1 (MCP-1). Furthermore, the transcription activity and nuclear translocation of NF-kB were found to be markedly decreased by WY-14643, while the phosphorylation of IkB was enhanced, indicating that the anti-inflammatory role of WY-14643 was meditated by NF-kB-dependent pathway. The application of WY-14643 failed to carry out its anti-inflammatory function in PPAR-α silenced cells, suggesting the role of PPAR-α. These findings may facilitate further studies investigating the translation of pharmacological PPAR-α activation into clinical therapy of OA.

Keywords WY-14643 · Osteoarthritis · Synovial fibroblasts · Inflammation · NF-kB

Introduction

Osteoarthritis (OA) is a major source of pain, crippling, and disability, mainly characterized by the degradation of articular cartilage and associated with subchondral bone lesions (Glyn-Jones et al. 2015; Hunt et al. 2014). It is usually caused by previous joint injury, abnormal joint or limb development, and inherited factors, affecting about 10 % of men and 18 % of women over 60 years of age (Woolf et al. 2003).

OA has been considered as a chronic disease, manifested by persistence of inflammatory responses, infiltration of lymphocytes in multiple joints, and activation of diverse innate inflammatory danger signals. Regulation of inflammation in joint has caught the attention of strategies designed for OA. A few treatment options for OA have been developed and used aiming at reducing pain and controlling inflammation to improve function, such as non-steroidal anti-inflammatory drugs and corticosteroid injections (Hochberg et al. 2012). A plenty of studies about the biotherapies of OA targeting inflammatory mediators, such as tumor necrosis factor-α (TNF-α), interleukin-6 (IL-6), and cyclooxygenase-2 (COX-2), have been evaluated (Chevalier et al. 2009; Cho et al. 2015; Pers et al. 2015). However, a majority of these strategies did not achieve the desired results.

Electronic supplementary material The online version of this article (doi:10.1007/s12031-016-0775-y) contains supplementary material, which is available to authorized users.

✉ Degang Huang
xuhg@medmail.com.cn

✉ Hongguang Xu
xuhg@medmail.com

[1] Department of Orthopedic Surgery, Yijishan Hospital, Wannan Medical College, Wuhu, Anhui, People's Republic of China

Synovium is a thin membrane lining the nonarticular surfaces of diarthrodial joints, consists of type A cells (macrophage) and type B cells (synovial fibroblast). Irritated, thickened, and inflamed synovium can be found in osteoarthritis. Under stimulation from infiltrated inflammatory cells, synovial fibroblast become a less effective lubricant of the cartilge surfaces by making smaller hyaluronan and also produce several types of cytokines (IL-1β, TNF-α), chemokines, adhesion molecules, and proteinases that can digest the cartilage extracellular matrix (Man et al. 2014; Seto et al. 2004). Therefore, therapies based on suppressing the inflammation of synovial fibroblast might bring more efficient treatment for patients with OA.

It has been demonstrated that nuclear receptor peroxisome proliferator-activated receptor alpha (PPAR-α) behaves as a modulator of both acute and chronic inflammation in several tissues, including vascular wall, heart, nervous tissue, lung, gut, and liver (Gervois and Mansouri 2012; Gervois et al. 2012; Hecker et al. 2015; Zambon et al. 2006). As a therapeutic target in inflammation-associated diseases and proved to be useful to ameliorate acute lung injury, activation of PPAR-α by its ligand has been reported to ameliorate dyslipidemia and lipopolysaccharide (LPS)-induced acute lung injury (Fu et al. 2003; Yoo et al. 2013). However, its role in synovial fibroblasts is still unknown. This study is aimed to investigate the effect of PPAR-α agonist (WY-14643) on LPS-induced inflammation in synovial fibroblasts and underlying mechanism.

Materials and Methods

Cell Culture and Transfection

Synovial fibroblasts were obtained from patients with osteoarthritis who underwent knee or hip surgery according to Luo SF (Luo et al. 2010). Informed consent was obtained from all patients. Synovial tissues were cut into small pieces and placed in 10 -cm dishes and incubated in DMEM/F-12 medium (Sigma-Aldrich, St. Louis, USA) containing 10 % FBS, 100 U/mL penicillin G, 100 mg/mL streptomycin, and 250 ng/mL fungizone at 37 °C in a humidified 5 % CO_2 atmosphere. When the cultures reached confluence, cells were digested with 0.05 % (*w*/*v*) trypsin/0.53 mM EDTA for 5 min at 37 °C and diluted with DMEM/F-12 containing 10 % FBS to a concentration of 2×10^5 cells/mL. Culture medium was changed every 3 days. Experiments were performed using cells from passages 4 to 5. Over 95 % of the cells were fibroblasts, which were characterized by an immunofluorescence staining using an antibody specific for a fibroblast protein vimentin (shown in supplement Fig. 1). For gene silencing, PPAR-α-specific siRNA and the scrambled siRNA were transfected into synovial fibroblasts using Lipofectamine 2000 according to the manufacturer's instructions, respectively. After 48 h, the cells were tested for gene knocking-down efficiency and followed by other treatments.

Western Blot

After stimulation, synovial fibroblasts were harvested and lysed in 1× RIPA (Cell Signaling Technology, Danvers, MA, USA) containing phosphatase and protease inhibitors (Sigma-Aldrich, St. Louis, MO, USA). The protein concentration was measured by BCA protein assay reagent obtained from Pierce, and 30 μg of protein samples were separated by 8 or 10 % SDS-polyacrylamide gel and transferred to nitrocellulose membranes (EMD Millipore, Billerica, MA, USA) by electroblotting. Then, the membranes were blocked with 5 % nonfat milk, followed by incubation with the primary antibody against PPAR-α, p-IkB, t-IkB, NF-kB-P50, NF-kB-P65, and β-actin at 4 °C overnight. The blots were then re-probed with horseradish peroxidase-conjugated second antibodies. The protein bands were detected by the enhanced chemiluminescence reagent (Pierce; Thermo Fisher) and examined by imaging systems (Bio-Rad, Hercules, CA, USA). All the antibodies were purchased from Cell Signaling Technology. Protein levels were analyzed in comparison to β-actin for each group by densitometry. Experiments were independently repeated three times.

Nuclear and Cytoplasmic Protein Extraction

After stimulation, cytoplasmic and nuclear proteins of synovial fibroblasts were extracted using Nuclear and Cytoplasmic Extraction Reagents obtained from Thermo Fisher strictly according to the manufacturer's instructions. Briefly, cells were harvested and washed with PBS after treatment and the supernatant was carefully removed, leaving the cell pellet as dry as possible. Ice-cold CER I (100 μL for 1×10^6 cells) was added in to fully suspend the cell pellet. And ice-cold CER II (5.5 μL for 1×10^6 cells) was added to the tube after 10-min incubation on ice. The tube was vortexed for 5 s on the highest setting and vortexed for another 5 s following 1-min incubation on ice. The tube was centrifuged for 5 min at maximum speed in a microcentrifuge (16,000×*g*) and the supernatant (cytoplasmic extract) to a clean prechilled tube and stored at −80 °C until use. The insoluble (pellet) fraction which contains nuclei was suspended by ice-cold NER (100 μL for 1×10^6 cells) and incubated on ice, vortexed on the highest setting for 15 s every 10 min, for a total of 40 min. Then, the tube was centrifuged for 10 min at maximum speed in a microcentrifuge and the supernatant (nuclear extract) to a clean prechilled tube and stored at −80 °C until use. The protein expression of NF-kB-P50, NF-kB-P65 in cytoplasm and nuclear was further determined by western blot.

Determine of NO Production

Synovial fibroblasts were treated with LPS (100 μg/mL) in the presence or absence of WY-14643. PPAR-α siRNA-transfected cells were also treated with LPS (100 μg/mL) together with WY-14643. After stimulation, the production of NO was determined using Griess reagents (Thermo Fisher). The procedure was performed in accordance with the manufacturer's instructions. Briefly, 300 μL of supernatant was mixed with 100 μL of Griess reagent and 2.6 mL of deionized water. The mixture was incubated for 30 min at room temperature, and the absorbance at 548 nm was measured. The concentrations of NO in the supernatants were calculated from a standard curve.

RNA Extraction and Quantitative Real-Time PCR

Total mRNA was extracted from synovial fibroblasts using the TRIzol reagent (Life Technologies), and complementary DNA was then reverse-transcripted from 1 μg of total RNA with reverse transcription kit (Takara Biotechnology Co., Ltd., Dalian, China) according to the manufacturer's instructions. PCR was performed using SYBR Green Master Mix (Takara Biotechnology Co., Ltd., Dalian, China), and GAPDH served as the internal control. The relative of expression levels of vascular cell adhesion molecule-1 (VCAM-1), intercellular cell adhesion molecule-1 (ICAM-1), ET-1, TF, COX-2, and inducible nitric oxide synthase (iNOS) were determined using the $2^{-\Delta\Delta Ct}$ method and shown as fold change over controls (Schefe et al. 2006). The primers are as follows: 5′-CGT GCC GCA CTG AAC TGG AC-3′ (forward) and 5′-CCT CAC ACT TCA CTG TCA CCT-3′ (reverse) for ICAM-1; 5′-ATT GGG AAA AAC AGA AAA GAG-3′ (forward) and 5′-GGC AAC ATT GAC ATA AAG T-3′ (reverse) for VCAM-1; 5′-TGC TCC TGC TCG TCC CTG ATG GAT-3′ (forward) and 5′-ATA ACG CTC TCT GGA GGG CTT-3′ (reverse) for ET-1; 5′-CTA GAA TTC TAC AAA TAC-3′ (forward) and 5′-ACG GAA TTC CCC TTT CT-3′ (reverse) for TF; 5′-TCA TCC ATA CAT CAA AT-3′ (forward) and 5′-GTG CAC TGT GTT TGG AGT-3′ (reverse) for COX-2; 5′-CAA GAG TTT GAC CAG AGG-3′ (forward) and 5′-TGG AAC CAC TCG TAC TTG-3′ (reverse) for iNOS; 5′-TGA AGG TCG GAG TCA ACG GAT TTG GT-3′ (forward) and 5′-CAT GTG GGC CAT GAG GTC CAC CAC′ (reverse) for GAPDH. All the primers were designed and synthesized by Sangon Biotech (Shanghai, China). The specificity of amplification was assessed by melting curve analysis and gel electrophoresis.

Enzyme-Linked Immunosorbent Assay (ELISA)

Concentrations of interleukin-6 (IL-6), tumor necrosis factor-α (TNF-α), monocyte chemotactic protein 1 (MCP-1), interleukin-1β (IL-1β), and prostaglandin E2 (PGE_2) in cell culture supernatant were determined by ELISA according to the manufacturer's instructions. ELISA kits for IL-6, TNF-α, MCP-1, and IL-1β were purchased from R&D systems (Germany). PGE_2 ELISA Kit was purchased from Abcam (Cambridge, MA, USA).

Luciferase Reporter Assays

To detect the activation of NF-kB, synovial fibroblasts were transfected plasmids encoding NF-kB responsive firefly luciferase and Renilla luciferase using Lipofectamine 2000. After transfection for 0, 3, or 12 h, cells were washed with phosphate-buffered saline, serum-starved in DMEM/F-12 overnight, and then assayed forluciferase activity using the dual-luciferase reporter assay kit (Promega Corporation, WI, USA). Briefly, the plate was incubated at 20–25 °C for 15 min after Dual-Glo® Luciferase assay reagent was added to the plate (75 μL/well). And the firefly luminescence was measured by automatic multi-mode microplate reader (infinite M200 pro, TeCan, Switzerland). After that Dual-Glo® Stop &Glo® reagent was added to the plate (75 μL/well) and followed by incubation at 20–25 °C for another 15 min, renilla luminescence in the same wells was detected by the same instrument. The ratio of firefly/renilla luminescence was calculated for each well. The sample well ratio was normalized to the ratio from a control wells.

Immunofluorescence Staining

After stimulation, synovial fibroblasts were washed with ice-cold PBS and fixed by 4 % paraformaldehyde at room temperature for 30 min. Blocking was performed with 3 % (*w*/*v*) bovine serum albumin (BSA) containing 0.1 % Triton X-100, 0.05 % Tween-20, and 10 % donkey serum for 2 h at room temperature to avoid unspecific staining. Then, the cells were incubated with the primary antibody for NF-kB-P50 (1:100) or NF-kB-P65 (1:100) overnight at 4 °C and followed by TRITC-conjugated secondary antibody and DAPI for 2 h at room temperature. After washing, cells were examined with Leica fluorescence microscope (Germany).

Data Analysis

Data represent the mean and standard error of the mean (SEM). Student's *t* test was performed for all statistical significance analysis using GraphPad Prism software (Version 5, GraphPad Software, Inc., La Jolla, CA). p Values <0.05 were considered statistically significant.

Results

WY-14643 Treatment Induces the Expression of PPAR-α in Synovial Fibroblasts

To examine the role of PPAR-α in the inflammation of synovial fibroblasts, the expression of PPAR-α was determined by western blot and quantitative real-time PCR following LPS and/or WY-14643 treatment. Protein expression of PPAR-α was slightly increased by 100 μg/mL LPS, but greatly enhanced by WY-14643 either in low or high concentration (Fig. 1a, b). In PPAR-α-specific siRNA-transfected cells, WY-14643 was unable to induce the expression of PPAR-α (Fig. 1a, b). Similar result was observed in the mRNA level (Fig. 1c).

WY-14643 In Vitro Treatment Decreases LPS-Induced Production of NO and PGE_2 in Synovial Fibroblasts

To demonstrate the effect of PPAR-α activation on inflammation of synovial fibroblasts, we first tested the production of NO and PGE_2, two indicators of the extent of the inflammatory response. As shown in Fig. 2a, b, WY-14643 effectively suppressed the production of both NO and PGE_2, comparing with LPS alone or PPAR-α silencing group. We also confirmed that the mRNA expression of iNOS and COX-2 was significantly inhibited by WY-14643 (Fig. 2c, d), the critical factors for the secretion of NO and PGE_2, respectively. These data indicated that WY-14643 might has suppressive effect in the inflammation in synovial fibroblasts by inhibiting the production of NO and PGE_2 at the transcriptional level.

PPAR-α Activation Suppresses the Expression of Inflammatory Factors Induced by LPS

To further confirm the role of WY-14643 in LPS-induced inflammation in synovial fibroblasts, expressions of series of inflammatory mediators were determined by quantitative real-time PCR. The expression of VCAM-1, ICAM-1, ET-1, and TF was strongly upregulated by LPS and significantly downregulated after being exposed to WY-14643 (Fig. 3), suggesting the inhibitive role of WY-14643 in LPS-induced inflammation in synovial fibroblasts.

PPAR-α Activation Reduces the Secretion of Pro-Inflammatory Cytokines Triggered by LPS

Next, we measured pro-inflammatory cytokines concentrations in cell culture supernatants by ELISA. We found enormous increases of IL-6, IL-1β, TNF-α, and MCP-1 levels in supernatants of synovial fibroblasts stimulated with LPS in comparison to unstimulated controls (Fig. 4). As expected, the concentrations of IL-6, IL-1β, TNF-α, and MCP-1 in cell supernatants following stimulation were greatly decreased by WY-14643 treatment (Fig. 4). However, the anti-inflammatory role of WY-14643 was not observed in PPAR-α silencing synovial fibroblasts.

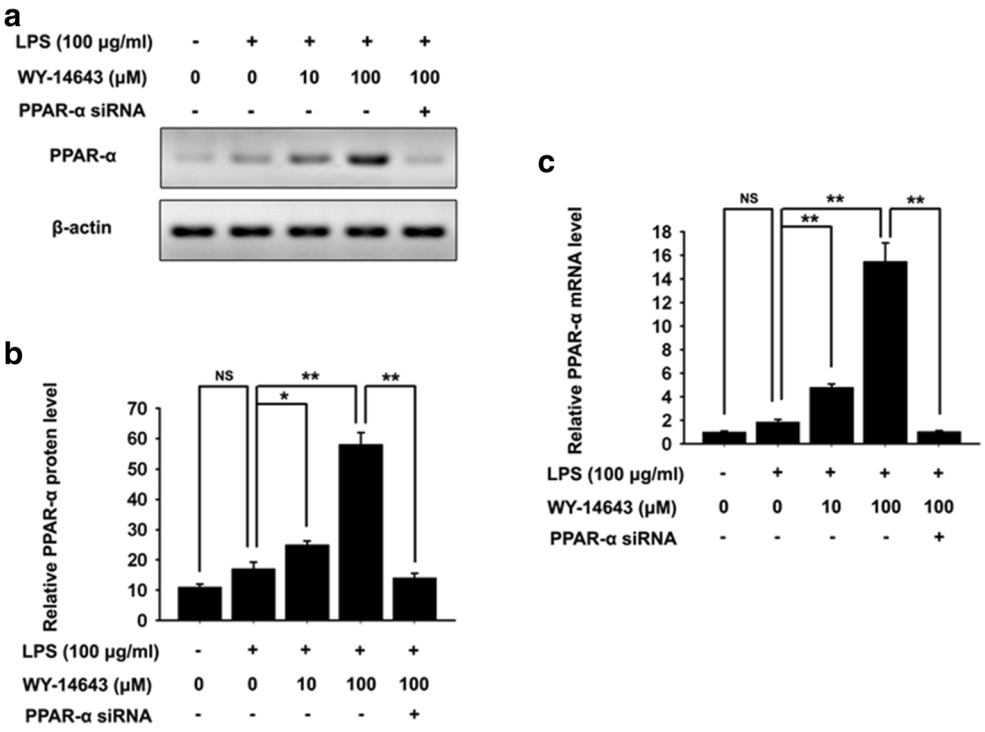

Fig. 1 Expression of PPAR-α in synovial fibroblasts following LPS treatment. Synovial fibroblasts were treated with different concentrations of LPS and WY-14643 for 24 h; cells were transfected with PPAR-α siRNA 48 h prior to treatment in *lane 5*. The protein level and mRNA level of PPAR-α was detected by western blot (**a**, **b**) and quantitative real-time PCR (**c**), respectively. Data are mean ± SEM for three independent experiments (*$p < 0.05$ and **$p < 0.01$ between the indicated groups)

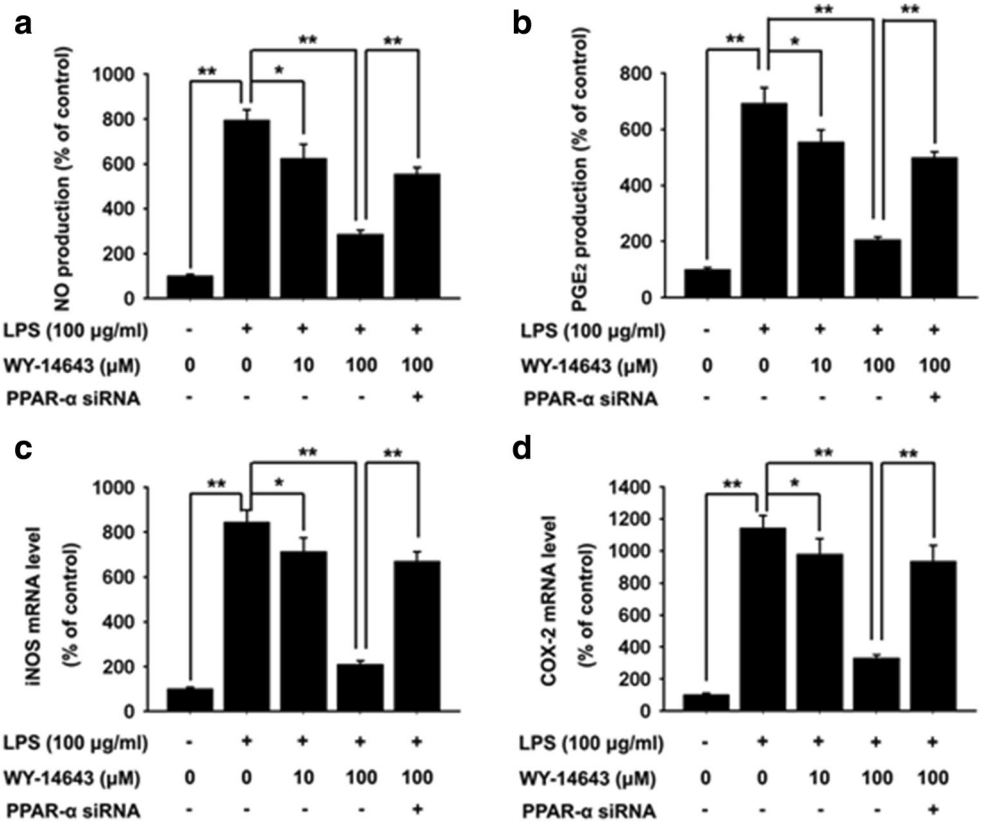

Fig. 2 Impact of WY-14643 and PPAR-α siRNA on NO and PGE_2 production in LPS-stimulated synovial fibroblasts. Synovial fibroblasts were treated with LPS (100 μg/mL) in the presence or absence of WY-14643 (0, 10, and 100 μM). PPAR-α siRNA-transfected cells were treated with LPS (100 μg/mL) together with WY-14643. After stimulation, culture supernatants were collected and the resultant concentrations of NO (**a**) and PGE_2 (**b**) were determined using the Griess assay and ELISA, respectively. Additionally, cells were harvested to extract total RNA and the relative iNOS (**c**) and COX-2 (**d**) mRNA expression was assessed by quantitative real-time PCR. Data are presented as mean ± SEM for three independent experiments (*$p < 0.05$ and **$p < 0.01$ between the indicated groups)

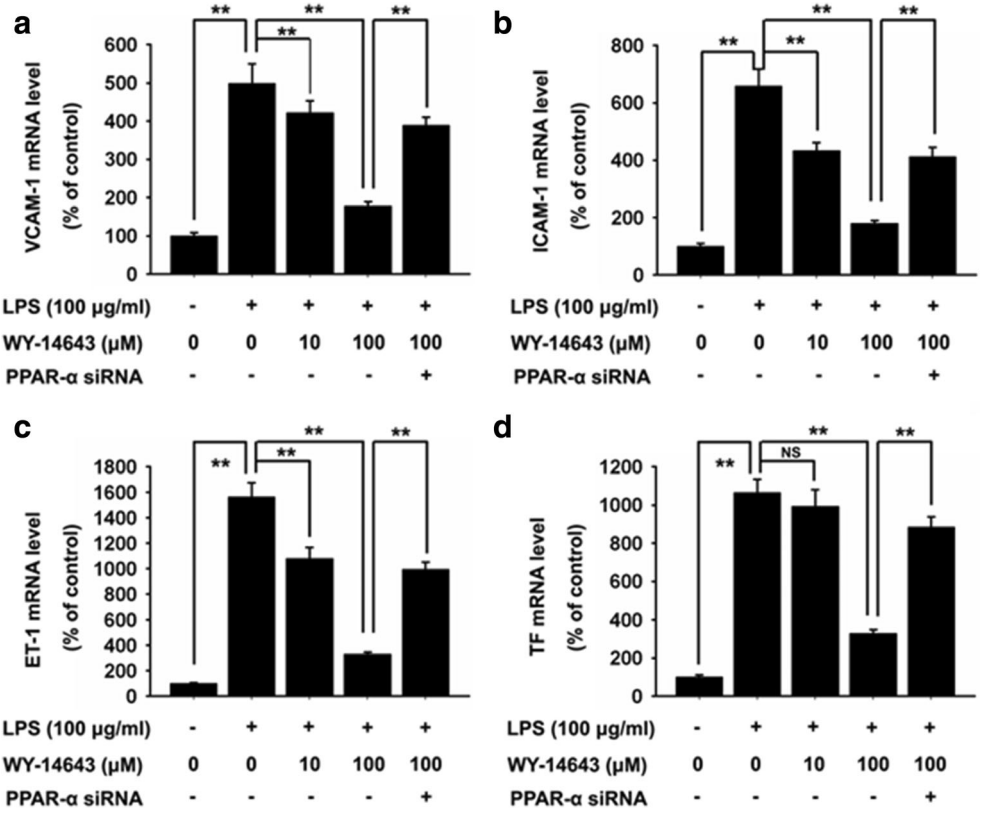

Fig. 3 Expression of inflammatory mediators in synovial fibroblasts following stimulation. After indicated stimulation, total RNA was extracted from synovial fibroblasts and the relative expression of VCAM-1 (**a**), ICAM-1 (**b**), ET-1 (**c**), and TF (**d**) was determined by quantitative real-time PCR. Relative mRNA expression was calculated using the $2^{-\Delta\Delta Ct}$ method and shown as percent change over controls. Data are mean ± SEM for three independent experiments (*$p < 0.05$ and **$p < 0.01$ between the indicated groups)

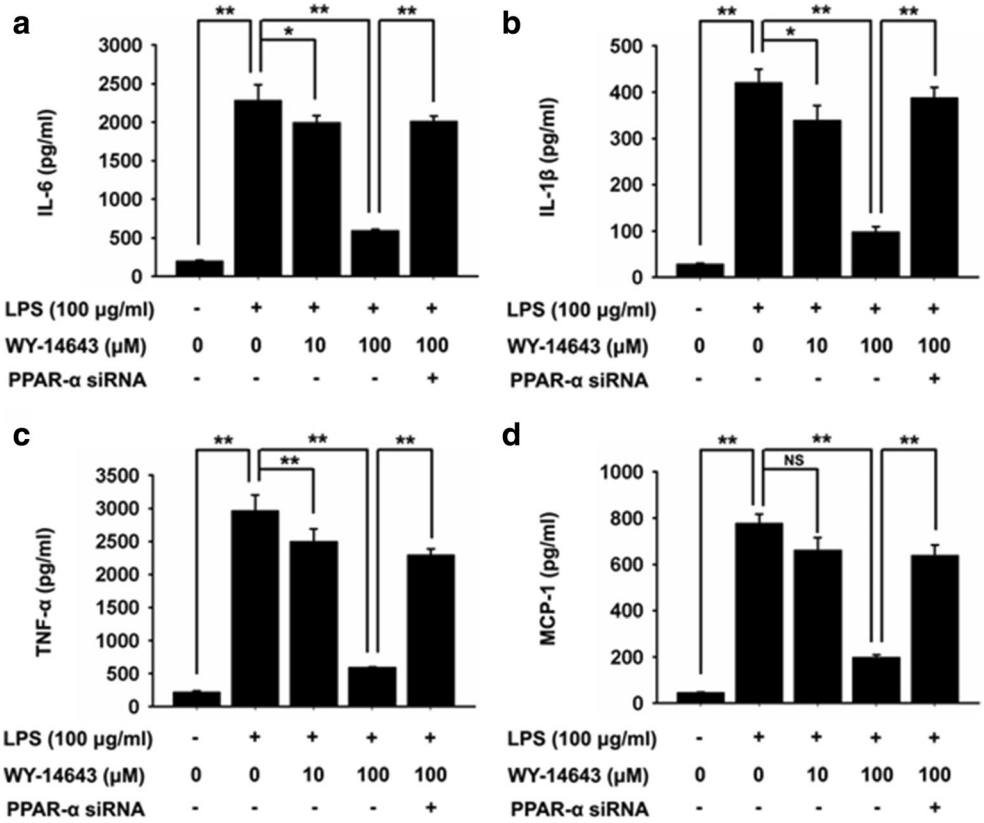

Fig. 4 Effects of PPAR-α on inflammatory cytokine secretion. After stimulated with indicated factors, culture supernatants of synovial fibroblasts were collected and the concentrations of IL-6, IL-1β, TNF-α, and MCP-1 in each group were detected by ELISA according to the manual. Data are presented as mean ± SEM for three independent experiments (*$p < 0.05$ and **$p < 0.01$ between the indicated groups)

PPAR-α Activation Inhibits LPS-Induced NF-kB Activation and IkB Phosphorylation

As mentioned above, the mRNA expression of series of inflammatory factors was markedly suppressed by WY-14643, suggesting that the anti-inflammatory role of WY-14643 might be mediated by a transcription factor. It is well known that inflammation is controlled by multiple signaling pathways in mammalian cells, in which NF-kB plays a pivotal role in the regulation of inflammatory responses. To explore if NF-kB is involved in the anti-inflammatory role of WY-14643, synovial fibroblasts were transfected with kB-luciferase expression vector prior to LPS and WY-14643 stimulation, transcription factor activity of NF-kB was assessed with a luciferase reporter gene assay. As expected, WY-14643 greatly suppressed the NF-kB luciferase activity induced by LPS (Fig. 5). Decreasing of phosphorylated IkB and increasing of total IkB protein level were also observed following WY-14643 treatment (Fig. 6), indicating that the phosphorylation, ubiquitination, and degradation of IkB induced by LPS was inhibited by WY-14643.

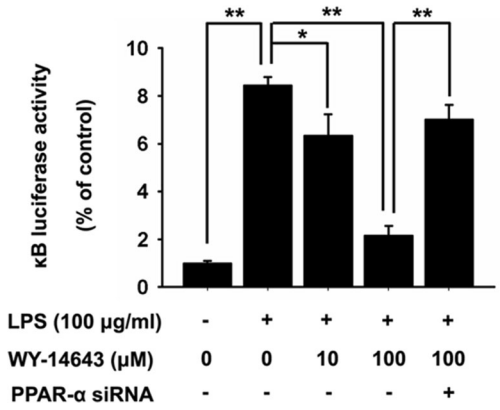

Fig. 5 WY-14643 inhibits LPS-induced NF-kB reporter activity. Synovial fibroblasts were transfected with kB-luciferase expression vector incubated with LPS with or without WY-14643. Luciferase activity was then measured. Note that WY-14643 greatly suppressed the kB-luciferase activity. Data are presented as mean ± SEM for three independent experiments (*$p < 0.05$ and **$p < 0.01$ between the indicated groups)

PPAR-α Activation Inhibits LPS-Induced NF-kB Nuclear Translocation

After dissociation from IkB, the activated NF-kB is then translocated into the nucleus where it binds to specific sequences of DNA to regulate the expression of downstream genes. In the next setting, we detected NF-kB nuclear translocation by western blot and immunofluorescence analysis. As shown in Fig. 7, LPS markedly increased the levels of p50 and p65 subunit in nuclear extract when compared to untreated cells. Interestingly, WY-14643 inhibited the

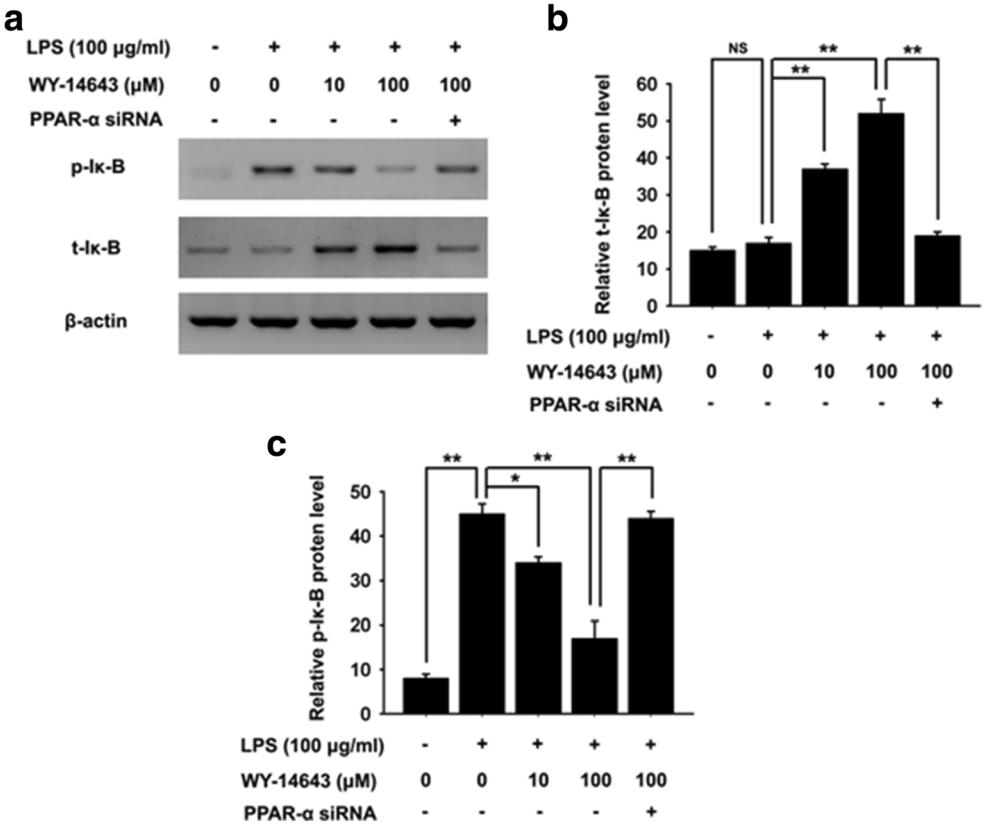

Fig. 6 Effect of WY-14643 on the activation of Ik-B. Expression and phosphorylation of Ik-B in synovial fibroblasts following LPS and WY-14743 was detected by western blot (**a**). Expression of t-IkB was markedly enhance by WY-14643 and inhibited by PPAR-α siRNA (**b**). LPS enhanced the phosphorylation of Ik-B and significantly suppressed by WY-14643 (**c**). Data are presented as mean ± SEM for three independent experiments (*$p < 0.05$ and **$p < 0.01$ between the indicated groups)

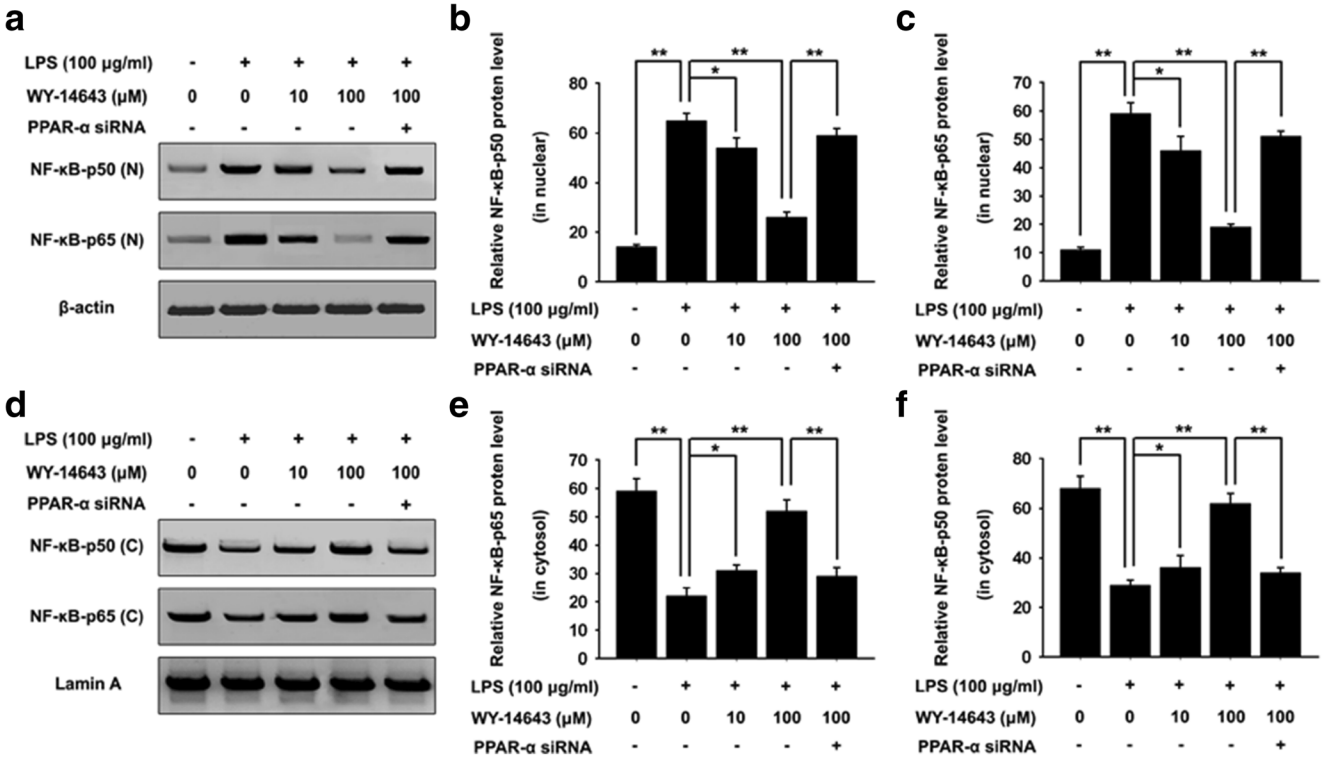

Fig. 7 Nuclear translocations of NF-*k*B-p50 and NF-*k*B-p65. After stimulating, synovial fibroblasts were harvested, cytoplasmic and nuclear protein extracted, respectively. The expression level of NF-kB-p50 and NF-kB-p65 in cytoplasm (**a**) and nuclear (**d**) was determined by western blot. The bar charts demonstrate the ratio of NF-kB-p50 and NF-kB-p65 protein relative to β-actin (**b**, **c**) or lamin A (**e**, **f**) for each group by densitometry. Data are presented as mean ± SD for three independent experiments (*$p < 0.05$ and **$p < 0.01$ between the indicated groups)

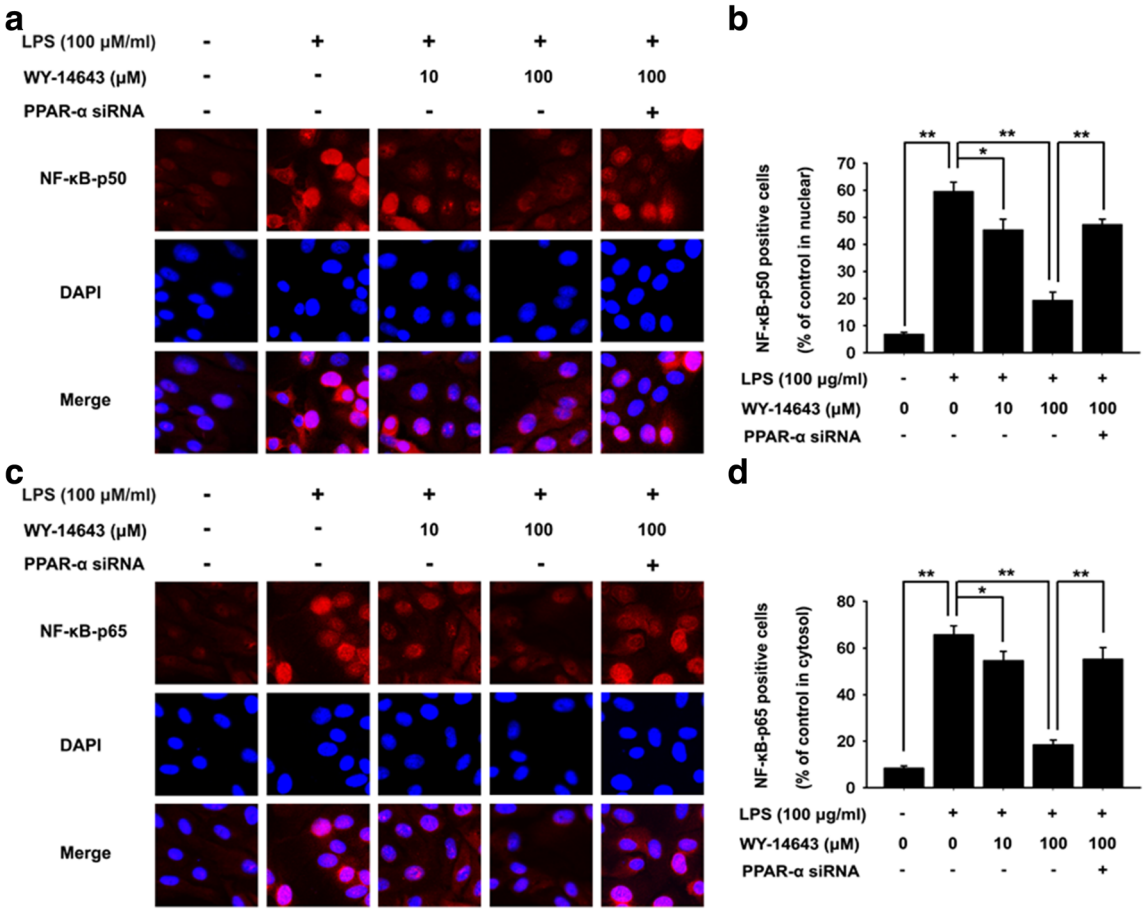

Fig. 8 Distribution of NF-kB-p50 and NF-kB-p65 in synovial fibroblasts. **a** Synovial fibroblasts were stained with NF-kB-p50 (*red*) and DAPI (*blue*) after stimulation and fixation. **b** Number of NF-kB-p50-positive cells was counted and showed as the ratio of control group. **c** Synovial fibroblasts were stained with NF-kB-p65 (*red*) and DAPI (*blue*). **c** Number of NF-kB-p65-positive cells was counted compared with control group. The images shown are representative of three experiments. Magnification ×400. Data are mean ± SD for three independent experiments (*$p < 0.05$ and **$p < 0.01$ between the indicated groups)

translocation of NF-kB subunits from cytosol into nucleus either in low or high concentration, but not in PPAR-α silenced synovial fibroblasts (Fig. 7a–f).

The inhibition of NF-kB translocation by WY-14643 was also confirmed by immunofluorescence staining (Fig. 8). The distributions of NF-kB-p50 and NF-kB-p65 in nucleus were boosted by LPS and reversed by WY-14643 in a dose-dependent way (Fig. 8a–c). However, there was no change of NF-kB nuclear translocation after WY-14643 treatment in PPAR-α silenced cells.

Discussion

Cartilage injury caused by various pathological conditions such as trauma, inflammation, and aging is always followed by osteoarthritic changes of the affected joints (Glyn-Jones et al. 2015). As the most common degenerative joint disorder, OA results in pain and loss of joint function and high costs for treating patients. Therefore, it is urgent to find out an efficient treatment for patients with OA by targeting the cells or molecules that regulate the pathological changes. There is increasing recognition that synovium become inflammatory in which synovial fibroblasts take an important role (Goldring et al. 2015; Qin et al. 2014), apart from the pathophysiological changes in cartilage and peri-articular bone (Pap et al. 2015). In this study, we demonstrated that PPAR-α agonist WY-14643 significantly reduced LPS-induced inflammation in synovial fibroblasts.

NO and PGE_2 levels have been demonstrated much higher in patients with OA and considered as diagnostic and prognostic biomarkers in clinical development of OA (Attur et al. 2015; de Lange-Brokaar et al. 2015). It is well known that iNOS and COX-2 are important regulatory inflammatory factors. After inflammatory stimulation, large amounts of pro-inflammatory mediators of NO and PGE_2 could be generated by iNOS and COX-2, respectively. In our experiments, the production of NO and PGE_2 in synovial fibroblasts was profoundly increased by 100 μg/mL LPS treatment, which is consistent with previous results. Interestingly, application of

WY-14643, which enhanced the expression of PPAR-α, greatly inhibited the generation of NO and PGE_2 induced by LPS in a dose dependent way. As expected, the increasing of iNOS and COX-2 in mRNA level was also found suppressed by WY-14643 treatment. This is the first report investigating the production of NO and PGE_2 in inflammatory synovial fibroblasts in response to WY-14643, we deduced that PPAR-α activation in synovial fibroblasts might inhibit its inflammatory response.

In support of the present findings, previous reports have described the inhibitory effects of PPAR agonists on inflammatory mediators in vivo and vitro experiments (Libby et al. 2007; Mutua et al. 2015; Pontis et al. 2016). In the present study, we measured the secretion of pro-inflammatory cytokines as the indicators for inflammatory response of synovial fibroblasts. The secretion of IL-6, IL-1β, TNF-α, and MCP-1 in cell supernatants induced by LPS was greatly decreased by WY-14643. The secretion of cytokines are in line with the production of NO and PGE_2 in inflammatory synovial fibroblasts, suggesting its anti-inflammatory potency.

It has been demonstrated that the level of soluble adhesion molecule VCAM-1 was positively associated with the number of affected joints of hand OA and emerged as a strong and independent predictor of the risk of hip and knee joint replacement due to severe OA (Kalichman et al. 2011; Schett et al. 2009). The expression of adhesion molecules contribute to the adhesiveness between synovial fibroblasts and immune cells, which promotes the infiltration of immune cells and aggravates the development of OA. Collagen-induced arthritis was greatly relieved in VCAM-1 deficiency mice (Carter et al. 2002). In our experiments, we found the mRNA expression of adhesion molecules VCAM-1, ICAM-1, ET-1, and TF in synovial fibroblasts was significantly increased after LPS treatment and inhibited by PPAR-α activation, indicating the potential protective role of PPAR-α agonist in the treatment of OA.

Since inflammation balance is important for the survival of cells, the precise regulation of inflammations in mammalian cells must be well achieved. To elucidate the mechanism underlying anti-inflammatory effect of WY-14643, we focused on the signaling pathways. It has been long appreciated that NF-kB is an important transcription factor that functions in immune and inflammatory responses (Brady et al. 2015; Columbano et al. 2005; Espin-Palazon et al. 2014), characterized by translocation from cytoplasm to nucleus and promoting the expression of pro-inflammatory mediators including iNOS, COX-2, IL-6, and TNF-α, which we have found greatly changed after LPS and WY-14643 stimulation. Therefore, we detected the activation of NF-kB in synovial fibroblasts. Luciferase report system showed the transcription activity of NF-kB induced by LPS was prevented by WY-14643. Activation of NF-kB is mainly mediated by phosphorylation and degradation of IkB, which permits NF-kB dissociate from IkB and enter the nucleus. Here, we found the phosphorylation of IkB caused by LPS was decreased by WY-14643, while the total protein level of IkB was restored. Nuclear and cytoplasmic protein was extracted to determine the translocation of NF-kB. Our data showed that LPS increased the translocation of NF-kB p50 and p65 from the cytoplasm into the nucleus, which is consistent with previous studies (Carneiro et al. 2013). As we have expected, application of WY-14643 increased the accumulation of NF-kB p50 and p65 in the cytoplasm and the nuclear translocation of NF-kB caused by LPS was interrupted. Consequently, the transcriptional regulation of NF-kB was impaired; the mRNA expression of downstream inflammatory target genes of NF-kB was remarkably decreased by WY-14643, including VCAM-1, ICAM-1, ET-1, and TF. These results confirmed that the prevention of IkB degradation and nuclear entry of NF-kB was involved in the anti-inflammatory effect of WY-14643 in synovial fibroblast. Importantly, the anti-inflammatory role of WY-14643 was not observed in PPAR-α silencing synovial fibroblasts, the production of inflammatory mediators and cytokines and the activation of NF-kB displayed no significant changes due to WY-14643 treatment, suggesting the anti-inflammation role of WY-14643 is dependent on the activation of PPAR-α.

In summary, the present study provided the direct evidence that PPAR-α agonist WY-14643 remarkably suppressed LPS-induced inflammatory responses in synovial fibroblasts, including the production of NO and PGE_2, secretion of pro-inflammatory cytokines and expression of inflammatory genes, and activation of NF-kB pathway. These results suggest that WY-14643 may be useful as a therapeutic agent against OA by inhibiting the inflammation in synovial fibroblasts.

Acknowledgments This study was supported by the National Natural Science Foundation of China (81572185,81272048,81311130314) and the Chinese Anhui Provincial Natural Science Foundation Project (1308085MH152).

References

Attur M et al (2015) Low-grade inflammation in symptomatic knee osteoarthritis: prognostic value of inflammatory plasma lipids and peripheral blood leukocyte biomarkers. Arthritis Rheumatol 67:2905–2915

Brady G et al (2015) Poxvirus protein MC132 from molluscum contagiosum virus inhibits NF-B activation by targeting p65 for degradation. J Virol 89:8406–8415

Carneiro AB et al (2013) Lysophosphatidylcholine triggers TLR2- and TLR4-mediated signaling pathways but counteracts LPS-induced NO synthesis in peritoneal macrophages by inhibiting

NF-kappaB translocation and MAPK/ERK phosphorylation. PLoS One 8:e76233
Carter RA et al (2002) Vascular cell adhesion molecule-1 (VCAM-1) blockade in collagen-induced arthritis reduces joint involvement and alters B cell trafficking. Clin Exp Immunol 128:44–51
Chevalier X et al (2009) Intraarticular injection of anakinra in osteoarthritis of the knee: a multicenter, randomized, double-blind, placebo-controlled study. Arthritis Rheum 61:344–352
Cho H et al (2015) Study of osteoarthritis treatment with anti-inflammatory drugs: cyclooxygenase-2 inhibitor and steroids. Biomed Res Int 2015:595273
Columbano A et al (2005) Gadd45beta is induced through a CAR-dependent, TNF-independent pathway in murine liver hyperplasia. Hepatology 42:1118–1126
de Lange-Brokaar BJ, et al. (2015) Characterization of synovial mast cells in knee osteoarthritis: association with clinical parameters. Osteoarthritis Cartilage
Espin-Palazon R et al (2014) Proinflammatory signaling regulates hematopoietic stem cell emergence. Cell 159:1070–1085
Fu J et al (2003) Oleylethanolamide regulates feeding and body weight through activation of the nuclear receptor PPAR-alpha. Nature 425: 90–93
Gervois P et al (2012) PPARalpha as a therapeutic target in inflammation-associated diseases. Expert Opin Ther Targets 16:1113–1125
Glyn-Jones S et al (2015) Osteoarthritis. Lancet 386:376–387
Goldring MB et al (2015) Emerging targets in osteoarthritis therapy. Curr Opin Pharmacol 22:51–63
Hecker M et al (2015) PPAR-alpha activation reduced LPS-induced inflammation in alveolar epithelial cells. Exp Lung Res 41:393–403
Hochberg MC et al (2012) American College of Rheumatology 2012 recommendations for the use of nonpharmacologic and pharmacologic therapies in osteoarthritis of the hand, hip, and knee. Arthritis Care Res (Hoboken) 64:465–474
Hunt LP et al (2014) 45-day mortality after 467,779 knee replacements for osteoarthritis from the National Joint Registry for England and Wales: an observational study. Lancet 384:1429–1436
Kalichman L et al (2011) Association between vascular cell adhesion molecule 1 and radiographic hand osteoarthritis. Clin Exp Rheumatol 29:544–546
Libby P et al (2007) Inflammation in diabetes mellitus: role of peroxisome proliferator-activated receptor-alpha and peroxisome proliferator-activated receptor-gamma agonists. Am J Cardiol 99: 27B–40B
Luo SF et al (2010) Involvement of MAPKs and NF-kappaB in tumor necrosis factor alpha-induced vascular cell adhesion molecule 1 expression in human rheumatoid arthritis synovial fibroblasts. Arthritis Rheum 62:105–116
Man GS et al (2014) Osteoarthritis pathogenesis - a complex process that involves the entire joint. J Med Life 7:37–41
Mutua MP et al (2015) Activation of peroxisome proliferator-activated receptor gamma induces anti-inflammatory properties in the chicken free avian respiratory macrophages. J Anim Sci Technol 57:40
Pap T et al (2015) Cartilage damage in osteoarthritis and rheumatoid arthritis–two unequal siblings. Nat Rev Rheumatol 11:606–615
Pers YM et al (2015) Mesenchymal stem cells for the management of inflammation in osteoarthritis: state of the art and perspectives. Osteoarthritis Cartilage 23:2027–2035
Pontis S et al (2016) Macrophage-derived lipid agonists of PPAR-alpha as intrinsic controllers of inflammation. Crit Rev Biochem Mol Biol 51:7–14
Qin Y et al (2014) HMGB1-LPS complex promotes transformation of osteoarthritis synovial fibroblasts to a rheumatoid arthritis synovial fibroblast-like phenotype. Cell Death Dis 5:e1077
Schefe JH et al (2006) Quantitative real-time RT-PCR data analysis: current concepts and the novel "gene expression's CT difference" formula. J Mol Med (Berl) 84:901–910
Schett G et al (2009) Vascular cell adhesion molecule 1 as a predictor of severe osteoarthritis of the hip and knee joints. Arthritis Rheum 60: 2381–2389
Seto H et al (2004) Distinct roles of Smad pathways and p38 pathways in cartilage-specific gene expression in synovial fibroblasts. J Clin Invest 113:718–726
Woolf AD et al (2003) Burden of major musculoskeletal conditions. Bull World Health Organ 81:646–656
Yoo SH et al (2013) Activation of PPARalpha by Wy-14643 ameliorates systemic lipopolysaccharide-induced acute lung injury. Biochem Biophys Res Commun 436:366–371
Zambon A et al (2006) Modulation of hepatic inflammatory risk markers of cardiovascular diseases by PPAR-alpha activators: clinical and experimental evidence. Arterioscler Thromb Vasc Biol 26:977–986